TITLE

Superconducting coincidence photon detector with short timing jitter

AUTHORS

S. Miki[1,2,*], S. Miyajima[1], M. Yabuno[1], T. Yamashita[3,4], T. Yamamoto[5], N. Imoto[5], R. Ikuta[5], R. A. Kirkwood[6], R. H. Hadfield[7], and H. Terai[1]

AFFILIATIONS

[1] *Advanced ICT Research Institute, National Institute of Information and Communications Technology, 588-2 Iwaoka, Nishi-ku, Kobe, Hyogo 651-2492, Japan*

[2] *Graduate School of Engineering Faculty of Engineering, Kobe University, 1-1 Rokkodai-cho, Nada, Kobe 657-0013, Japan*

[3] *Graduate School of Engineering, Nagoya University, Furo-cho, Chikusa-ku, Nagoya 464-8603, Japan*

[4] *PRESTO, Japan Science and Technology Agency, 4-1-8 Honcho, Kawaguchi, Saitama 332-0012, Japan*

[5] *Graduate School of Engineering Science, Osaka University, Toyonaka, Osaka 560-8531, Japan*

[6] *National Physics Laboratory, Hampton Road, Teddington, TW11 0LW, UK*

[7] *School of Engineering, University of Glasgow, Glasgow G12 8LT, UK*

ABSTRACT

We demonstrate the operation of a coincidence photon detector with short timing jitter consisting of two superconducting nanowire single photon detectors (SSPDs) and a single flux quantum (SFQ) circuit. By utilizing the timing discrimination capability of the SFQ coincidence circuit, the full width at half maximum (FWHM) timing jitter of the entire coincidence photon detector was evaluated as 32.3 ps, which is 36 ps less than that of the standard commercial time correlated single photon counting (TCSPC) module, and the timing jitter of the SSPD was estimated as ~15 ps. Owing to short timing jitter characteristics, our coincidence photon detector could correctly capture the effect of pulse-width broadening by insertion of an optical bandpass filter. We have also demonstrated that our coincidence photon detection clearly shows Hong-Ou-Mandel (HOM) interference with a weak coherent pulse. These results are a crucial step to realizing high timing resolution coincidence measurements, ushering in a technology for timing measurement based multi-photon quantum interference.

TEXT

In the field of photonic quantum information technology, the Hong-Ou-Mandel (HOM) effect between indistinguishable photons[1] underpins a range of components and protocols in photonic quantum technologies[2], including quantum interfaces[3,4], quantum repeaters[5,6] and quantum secure communications[7,8]. As the performance of the HOM interference measurement for quantum technologies depends on the detection efficiency (DE), dark count rate (DCR), and the timing jitter of single photon detectors, detectors satisfying these requirements are strongly desired. Especially if the contribution of the timing jitter of the photon detectors is smaller than the coherence time of photons, the timing measurement reveals HOM interference even with asynchronous photon sources, for example, continuous wave (CW) pumped spontaneous parametric down conversion (SPDC)[9]. Conventionally HOM measurements have been performed using pulse-pumped SPDC to enable precise timing control of photon-pair generation.

Superconducting nanowire single photon detectors (SSPDs)[10] are promising for HOM observation because of the high DE of ~90%[11], low DCR of a few counts/s[12], and short timing jitter as low as ~20 ps with a Gaussian instrumental response[13]. Successful observations of HOM interference using SSPDs have been demonstrated [3,4,9,14,15]. Meanwhile, the measured timing jitter of SSPD systems still has potential for improvement by suppressing external contributions other than the intrinsic jitter of detector itself, such as the contributions of the low noise amplifier and time correlated single-photon counting (TCSPC) module. Signal deterioration due to signal propagation over several meters of low thermal conductivity coax to extract a signal from a cryogenic environment also causes an increase in timing jitter. Although the employment of semiconductor cryogenic amplifiers is an effective approach to avoid the signal deterioration and reduce the timing jitter of the SSPD system[16], it would be difficult to scale up with the number of SSPD channels because the same number of output cables and amplifiers must be installed into the cryocooler system. Meanwhile, single-flux-quantum (SFQ) circuits are promising candidates for SSPD readout electronics offering short timing jitter and scalability against the number of SSPD channels due to SFQ's small power consumption and reduced requirement for output cables[17-19]. In this work, we propose a superconducting coincidence photon detector consisting of two SSPDs and a SFQ coincidence circuit[20] which can considerably suppress the external contributions as compared to conventional room temperature readout electronics. The SFQ coincidence circuit is based on

superconducting single-flux-quantum (SFQ) comparator which has timing jitter as low as 1 ps[20], and the SFQ circuit can connect with the SSPD without signal amplification in a cryogenic environment below ~4 K, allowing reduction of the extrinsic timing jitter contributions. We implemented a superconducting coincidence photon detector in a 0.1 W GM cryocooler system and evaluated the timing jitter characteristics of the coincidence photon detector system. The coincidence photon counting capability was then demonstrated by the observation of HOM interference.

The SFQ coincidence circuit used in this work is almost the same as that reported in Ref. 20, except for the duration of the time window. The detailed configuration and systematic characterization of the circuit itself were described in Ref. 20, and the modified time window will be described later in this paper. We present a simplified schematic block diagram of the SFQ coincidence circuit and examples of circuit behavior for different timing relations between two input signals in Fig. 1(a) and (b), respectively. As shown in the figure, the SFQ coincidence circuit has two input ports – START and STOP – each of which are connected to the SSPD. The output signals of SSPDs are converted into SFQ pulses of amplitude ~0.5 mV and duration 4 ps by interface circuits called magnetically coupled DC/SFQ (MC-DC/SFQ) converters[17]. The pulses are propagated through a Josephson transmission line (JTL) to the SFQ comparator to differentiate the relative timing of input pulses between START′ and STOP′. An output SFQ pulse appears from the SFQ comparator only when an SFQ pulse arrives at the STOP′ port within 800 ps after an SFQ pulse arrives at the START′ port of the SFQ comparator, indicating the SFQ comparator acts as a coincidence circuit with a time window of 800 ps. The time window was set to be relatively long value of 800 ps in this experiment to facilitate the timing adjustment of START and STOP signals, but it can be arbitrarily set within a range of values by adjusting the time delay determined by the length of JTLs. The output SFQ pulses are then converted to rectangular pulses with an amplitude of ~2.0 mV and a duration of ~1.6 ns by the voltage driver circuit for detecting room temperature electronics. The power consumption of the SFQ coincidence circuit is ~190 μW, which is sufficiently small that its operation hardly affects the SSPD operation even if the SFQ coincidence circuit is located close to the SSPD.

To realize coincidence photon detection, we implemented two fiber-coupled NbTiN-SSPDs and an SFQ coincidence circuit in a 0.1 W GM cryocooler system operating at 2.4 K. We first investigated the timing jitter characteristics by utilizing the timing discrimination capability of the SFQ coincidence circuit. The experimental setup is shown in Fig.

1 (c). The two SSPDs used in this work comprise 10 nm-thick and 100 nm-wide NbTiN nanowire meandering structure covering an area of 15 × 15 μm^2 integrated with an optical cavity structure. They have a relatively higher switching current I_{sw} of ~48 μA than the standard devices (5-nm-thick, and 100-nm-wide NbTiN nanowire with I_{sw} of 18-20 μA)[21] because thicker nanowires are used to obtain a high signal-to-noise ratio in the output waveform, and hence, short timing jitter. As a result of the increased nanowire thickness, single-photon sensitivity is somewhat reduced and the system detection efficiency (SDE) has a lower value of 23% compared to our standard devices[21]. The bias currents applied to the SSPDs are 35 μA and 38 μA which were the optimum values for correct operation of the MC-DC/SFQ converters, respectively. Although the SDE of the devices at this bias current was only a few percent, optimization of the design of the MC-DC/SFQ converters can increase the maximum current sensitivity resolving this problem. The observed full width at half maximum (FWHM) timing jitters of the SSPDs were 37 ps and 38 ps respectively in the preliminary timing correlation measurement using low noise amplifiers located at room temperature (LNA 545, RF Bay Inc.) and the standard TCSPC module (Hydra harp 400, PicoQuant GmbH). The incident light from a mode-locked pulsed fiber laser with ~0.1 ps pulse width and 10 MHz repetition frequency (Calmer laser, Inc) was attenuated to a single photon level and split into two optical paths by using a 1 × 2 fiber splitter. The incident photons from each optical path enter the respective SSPDs through the variable optical delay line ranging from 0 to 400 ps with 0.01 ps resolution which can control the arrival timing of incident photons to the SSPDs, and the polarization controller to optimize the polarization conditions to achieve maximum counts in the SSPDs.

As described above, the probability of an output pulse being generated by the SFQ coincidence circuit is determined by the relative arrival times of SFQ input pulses between START and STOP. Therefore, by sweeping the relative timing, we can observe the transition of output probability, reflecting the convolution of timing jitters for two SSPDs and other external contributions. We swept the photon arrival time to the SSPD on the START input port by using the variable optical delay line and recorded the number of the output counts from the SFQ circuit, while the arrival time of incident photons to the SSPD on the STOP input port and the variable delay line in the SFQ circuit were fixed at appropriate values. Figure 2 shows the output count number as a function of photon arrival time on the START input port. The clear and sharp transition was observed as expected, and the Gaussian distribution was obtained from

the derivative of its sigmoidal fitting as shown in Fig. 3. The timing correlation between two SSPDs was also measured using the standard TCSPC module, which is also shown in the Fig. 3 for comparison. The FWHM jitter of our coincidence photon detector was estimated as 32.3 ps, which is clearly smaller than 68.3 ps obtained with the standard TCSPC module. It is apparent that improvement in the timing jitter could be achieved by reducing external contributions other than the essential timing jitter of SSPD. From the configuration of the experimental setup and possible jitter contributions, the observed jitter j_{obs} can be expressed as follows:

$$j_{obs}^2 = 2j_{SSPD}^2 + 2j_{photon}^2 + 2j_{MC-DC/SFQ}^2 + j_{comp}^2 \quad (1)$$

Here, the j_{SSPD}, j_{photon}, $j_{MC\text{-}DC/SFQ}$, and j_{comp} are the timing jitter contributions of the SSPD, photon arrival time, MC-DC/SFQ converter, and SFQ comparator, respectively. The contribution j_{photon} originates from the pulsed laser source, for which the factory-tested timing jitter is ~60 fs, which is almost negligible in this experiment. Careful investigation using electrical input signals with similar amplitude and rising slope as those of the SSPDs revealed that $j_{MC\text{-}DC/SFQ}$ is ~17ps[20]. We also measured j_{comp} individually as ~2.6 ps[20]. By utilizing these values, j_{SSPD} can be estimated as 14.8 ps, which is consistent with the values reported elsewhere[13] in spite of the fact that our device has a relatively large sensitive area. The contributions of timing jitter, as described above, indicate that improvement in j_{SSPD} and $j_{MC\text{-}DC/SFQ}$ are crucial for further improvement of the observed system jitter j_{obs}. Furthermore, j_{SSPD} originates from various factors such as hotspot formation dynamics in the local area of the nanowire ($j_{hotspot}$), fluctuation of resistance values by photon absorption (j_r)[22], difference in time delay depending on the location where the photons are absorbed in the meandering nanowire (j_g)[23]. In our devices, j_g is not negligible owing to the relatively large sensitive area of 15 μm × 15 μm and can be reduced further by using advanced measurement techniques, such as simultaneously detecting both parts of the electrical pulse as they propagate in opposite directions to the sides of the detector[23], thus compensating for the geometrical timing difference. The systematic and analytical investigation of $j_{hotspot}$ has also reported to reveal the physical mechanism of this jitter, giving a fruitful insight to improve j_{SSPD} further[24,25]. The value of $j_{MC\text{-}DC/SFQ}$ may be determined by two possible contributions: one originates from the electronic input signal and the other from the conversion process from the electrical signal to SFQ pulse. As the contribution from the electrical input signals is mainly determined by the rate of change of voltage at the discrimination level and the signal-to-noise ratio, SSPD devices with large I_{sw} will be effective for reducing this contribution. However, devices with

high I_{sw} tend to have lower DE, which must be resolved for use in quantum information technology and will be addressed in the next study. Regarding the jitter contribution from the process of conversion to an SFQ pulse, we believe that it is possible to reduce this effect by changing the design of the input transformer and/or increasing the dumping resistors in parallel with the Josephson junctions.

To demonstrate the validity of the evaluation method for timing jitter, we measured the transition curves of the output probabilities of the SFQ coincidence circuit with and without an optical band pass filter, which was inserted between the pulsed laser and the attenuators. The obtained Gaussian curves are shown in Fig.4. The FWHM jitter with the optical band pass filter is estimated as 55.4 ps, which is clearly larger than 32.7 ps obtained without the filter. This result can be explained well by the pulse-width broadening phenomena based on the law of Fourier transform of limited pulses; according to this law, the product of pulse Δt and spectral width $\Delta \nu$ exceeds ~0.441 for Gaussian pulses. Since we used an optical filter of 0.11 nm bandwidth (FWHM) at 1550 nm center wavelength, the minimum optical pulse width can be estimated as 31.55 ps. Meanwhile, the timing jitter of incident photon arrival time with an optical filter $j_{photon,filter}$ can be estimated as 31.6 ps by considering the observed timing jitter and using equation (1). The fact that the minimum pulse width determined by the Fourier-transform-limit agrees well with $j_{photon,filter}$ estimated from the observed jitter shows convincingly that the timing jitter evaluation method can accurately measure the timing jitter of the entire experimental setup, and can easily resolve the ~30 ps of additional jitter.

Finally, we demonstrated the coincidence photon counting capability via an observation of two-photon interference with classical photon sources. Figure 5 (a) shows the experimental setup for the two-photon interference observation. The incident light from the pulsed laser was attenuated to the single photon level (< 1 photon/pulse) and split into two optical paths by the 1 × 2 fiber splitter. Two-photon interference was performed by connecting the system to a 2 × 2 fiber coupler. The timing of photons entering the coupler was varied by means of the optical delay line located between the splitter and the coupler. The photons emerging from the two coupler outputs were sent to the optical inputs of the two SSPDs through SM fiber and a polarization controller. A longer optical fiber was placed before the SSPD on the STOP side to ensure photons entering the START side would always arrive first. We recorded the output counts as a function of the relative time delay between the two input ports of the fiber coupler by varying the optical delay line. The obtained results are shown in Fig. 5(b). As shown in the figure, a clear dip due to two-photon

interference was observed. The visibility of the dip was approximately half, which would be expected because weak coherent pulses were used in the experiment. The results verify that our coincidence photon detector can be used to observe two-photon interference, which can be applied for observing the non-classical properties of light.

In conclusion, we developed a coincidence photon detector by utilizing two fiber-coupled NbTiN-SSPDs integrated with an SFQ coincidence circuit in a GM cryocooler system. We observed the transition of the output signal generation probability from the SFQ coincidence circuit by varying the relative timing of incident photon arrival between two NbTiN-SSPDs, and the timing jitter of the entire coincidence photon detector was evaluated from the derivative of the transition curve. The obtained FWHM jitter was 32.3 ps, which is clearly smaller than the values obtained with the standard TCSPC module because of the reduction of external jitter contributions other than those due to the two SSPDs. The jitter from the SSPD, i.e., j_{SSPD} was estimated as 14.8 ps by extracting the contribution from other factors, and the value was consistent with other reported results[13]. We also observed that j_{obs} varies with the addition of the optical bandpass filter, which can be consistently explained by the pulse-width broadening phenomena based on the law of Fourier transform of limited pulses, indicating the correctness of our timing jitter evaluation method. Finally, we observed classical two-photon interference with the expected visibility, certifying the capability of our device as a coincidence photon detector even for HOM interference. The next step is to reduce the time window to a value less than the coherence time of photons; this can be easily realized as described earlier, and the further improvement of overall system timing jitter, enabling the realization of an extremely high time resolution coincidence photon detector for HOM interference observation with CW-pumped photon pairs. It is also noted that the SFQ coincidence circuit could be scaled up for higher order coincidence measurements because the number of cables required for SFQ circuit operation does not increase as the number of SSPD channels and its power consumption can be reduced further by employing the low-power SFQ circuit technology such as low-voltage RSFQ[26], ERSFQ[27], RQL[28] and AQFP[29], which would be useful for the measurement of higher order photon states.

ACKNOWLEDGEMENTS

This work was partly supported by the JSPS Grant-in-Aid for Scientific Research Grant Number JP16H02214 and JST CREST Grant Number JPMJCR1671. The SFQ devices were fabricated in the clean room for analog-digital superconductivity (CRAVITY) in National Institute of Advanced Industrial Science and Technology (AIST). RAK thanks the National Institute of Information and Communications Technology (NICT) for support through a research internship.

REFERENCES

[1]C. K. Hong, Z. Y. Ou, and L. Mandel, Phys. Rev. Lett. **59**, 2044 (1987).

[2]J.-W. Pan, Z.-B. Chen, C.-Y. Lu, H. Weinfurter, A. Zeilinger, and M. Żukowski, Rev. Mod. Phys. 84, 777 (2012).

[3]Rikizo Ikuta, Hiroshi Kato, Yoshiaki Kusaka, Shigehito Miki, Taro Yamashita, Hirotaka Terai, Mikio Fujiwara, Takashi Yamamoto, Masato Koashi, Masahide Sasaki, Zhen Wang, and Nobuyuki Imoto, Physical Review A **87**, 010301 (2013).

[4]Rikizo Ikuta, Toshiki Kobayashi, Hiroshi Kato, Shigehito Miki, Taro Yamashita, Hirotaka Terai, Mikio Fujiwara, Takashi Yamamoto, Masato Koashi, Masahide Sasaki, Zhen Wang, and Nobuyuki Imoto, Physical Review A **88**, 042317 (2013).

[5]N. Sangouard, C. Simon, H. de Riedmatten, and N. Gisin, Rev. Mod. Phys. **83**, 33 (2011).

[6]J. Hofmann, M. Krug, N. Ortegel, L. Gerard, M. Weber, W. Rosenfield, H. Weinfurter, Science **337**, 72 (2012).

[7] J. L. O'Brien, A. Furusawa, and J. Vučković, Nature Photonics **3**, 687 (2009).

[8] M. Sasaki, M. Fujiwara, H. Ishizuka, W. Klaus, K. Wakui, M. Takeoka, S. Miki, T. Yamashita, Z. Wang, A. Tanaka, K. Yoshino, Y. Nambu, S. Takahashi, A. Tajima, A. Tomita, T. Domeki, T. Hasegawa, Y. Sakai, H. Kobayashi, T.

Asai, K. Shimizu, T. Tokura, T. Tsurumaru, M. Matsui, T. Honjo, K. Tamaki, H. Takesue, Y. Tokura, J. F. Dynes, A. R. Dixon, A. W. Sharpe, Z. L. Yuan, A. J. Shields, S. Uchikoga, M. Legre, S. Robyr, P. Trinkler, L. Monat, J. B. Page, G. Ribordy, A. Poppe, A. Allacher, O. Maurhart, T. Langer, M. Peev, and A. Zeilinger, Opt Express **19**, 10387 (2011).

[9]Y. Tsujimoto, Y. Sugiura, M. Tanaka, R. Ikuta, S. Miki, T. Yamashita, H. Terai, M. Fujiwara, T. Yamamoto, M. Koashi, M. Sasaki, and N. Imoto, Opt Express **25**, 12069 (2017).

[10]G. N. Gol'tsman, O. Okunev, G. Chulkova, A. Lipatov, A. Semenov, K. Smirnov, B. Voronov, A. Dzardanov, C. Williams, and R. Sobolewski, Applied Physics Letters **79**, 705 (2001).

[11]F. Marsili, V. B. Verma, J. A. Stern, S. Harrington, A. E. Lita, T. Gerrits, I. Vayshenker, B. Baek, M. D. Shaw, R. P. Mirin, and S. W. Nam, Nature Photonics **7**, 210 (2013).

[12]S. Miki, M. Yabuno, T. Yamashita, and H. Terai, Opt Express **25**, 6796 (2017).

[13]J. Wu, L. You, S. Chen, H. Li, Y. He, C. Lv, Z. Wang, and X. Xie, Appl Opt **56**, 2195 (2017).

[14]Toshiki Kobayashi, Rikizo Ikuta, Shuto Yasui, Shigehito Miki, Taro Yamashita, Hirotaka Terai, Takashi Yamamoto, Masato Koashi, and Nobuyuki Imoto, Nature Photonics **10**, 441 (2016).

[15]R. B. Jin, M. Fujiwara, R. Shimizu, R. J. Collins, G. S. Buller, T. Yamashita, S. Miki, H. Terai, M. Takeoka, and M. Sasaki, Sci. Rep. **6**, 36914 (2016).

[16]I. E. Zadeh, J. W. N. Los, R. B. M. Gourgues, V. Steinmetz, G. Bulgarini, S. M. Dobrovolskiy, V. Zwiller, and S. N. Dorenbos, APL Photonics **2,** 111301 (2017).

[17]H. Terai, S. Miki, and Zhen Wang, IEEE Trans. on Appl. Supercond. **19**, 350 (2009).

[18] T. Ortlepp, M. Hofherr, L. Fritzsch, S. Engert, K. Ilin, D. Rall, H. Toepfer, H. G. Meyer, and M. Siegel, Opt. Express **19**, 18593 (2011).

[19]H. Terai, T. Yamashita, S. Miki, K. Makise, and Z. Wang, Opt. Exp. **20**, 20115 (2012).

[20] Shigeyuki Miyajima, Shigehito Miki, Masahiro Yabuno, Taro Yamashita, and Hirotaka Terai, Supercond. Sci. Technol. **30**, 12LT01 (2017).

[21]S. Miki, T. Yamashita, H. Terai, and Z. Wang, Opt Express **21**, 10208 (2013).

[22]J. A. O'Connor, M. G. Tanner, C. M. Natarajan, G. S. Buller, R. J. Warburton, S. Miki, Z. Wang, S. W. Nam, and R. H. Hadfield, Appl. Phys. Lett. **98**, 201116 (2011).

[23]Niccolò Calandri, Qing-Yuan Zhao, Di Zhu, Andrew Dane, and Karl K. Berggren, Appl. Phys. Lett. **109**, 152601 (2016).

[24]M. Sidorova, A. Semenov, H.-W. Hübers, I. Charaev, A. Kuzmin, S. Doerner, and M. Siegel, Physical Review B **96**, 184504 (2017).

[25]B. A. Korzh, Q-Y. Zhao, S. Frasca, J. P. Allmaras, T. M. Autry, E. A. Bersin, M. Colangelo, G. M. Crouch, A. E. Dane, T. Gerrits, F. Marsili, G. Moody, E. Ramirez, J. D. Rezac, M. J. Stevens, E. E. Wollman, D. Zhu, P. D. Hale, K. L. Silverman, R. P. Mirin, S. W. Nam, M. D. Shaw and K. K. Berggren, arXiv:1804.06839 (2018).

[26]M. Tanaka, M. Ito, A. Kitayama, T. Kouketsu and A. Fujimaki, Jpn. J. Appl. Phys. **51**, 053102 (2012).

[27]D. Kirichenko S. Sarwana, A. F. Kirichenko, IEEE Trans. on Appl. Supercond. **21**, 776 (2011).

[28]Q. P. Herr, A. Y. Herr, O. T. Oberg, and A. G. Loannidis, J. Appl. Phys. **109**, 103903 (2011).

[29] N. Takeuchi, T. Yamashita, S. Miyajima, S. Miki, N. Yoshikawa, H. Terai, Opt. Exp. **25**, 32650 (2017).

FIGURES

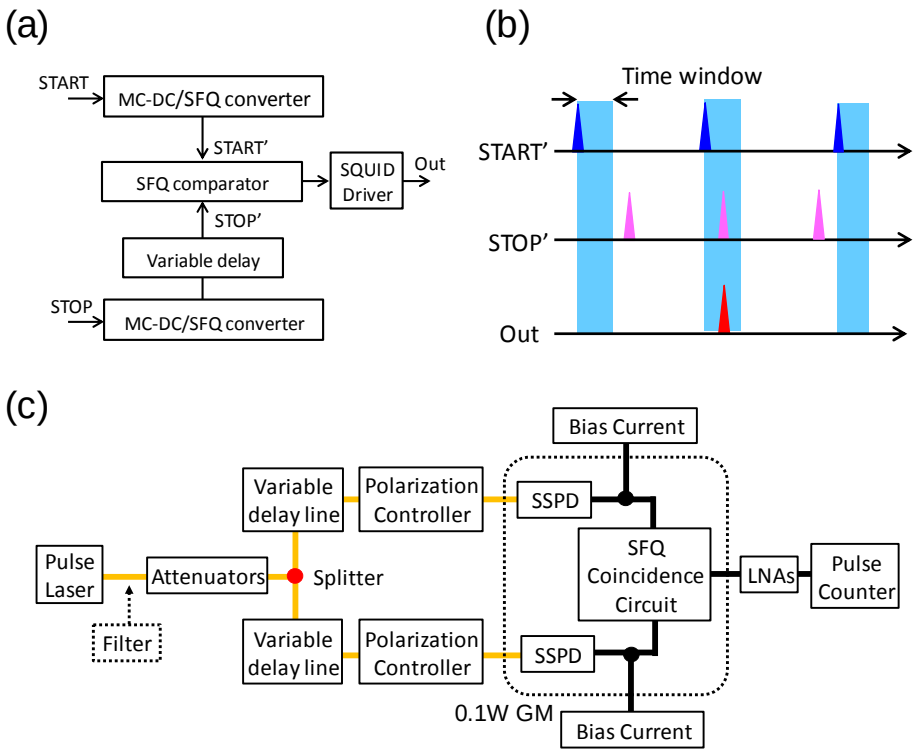

Fig. 1 (a) Schematic block diagram of the SFQ coincidence circuit. (b) Examples of timing relation between two input signals and output signal. (c) Experimental setup for timing correlation measurement between two SSPDs with the SFQ timing discriminator.

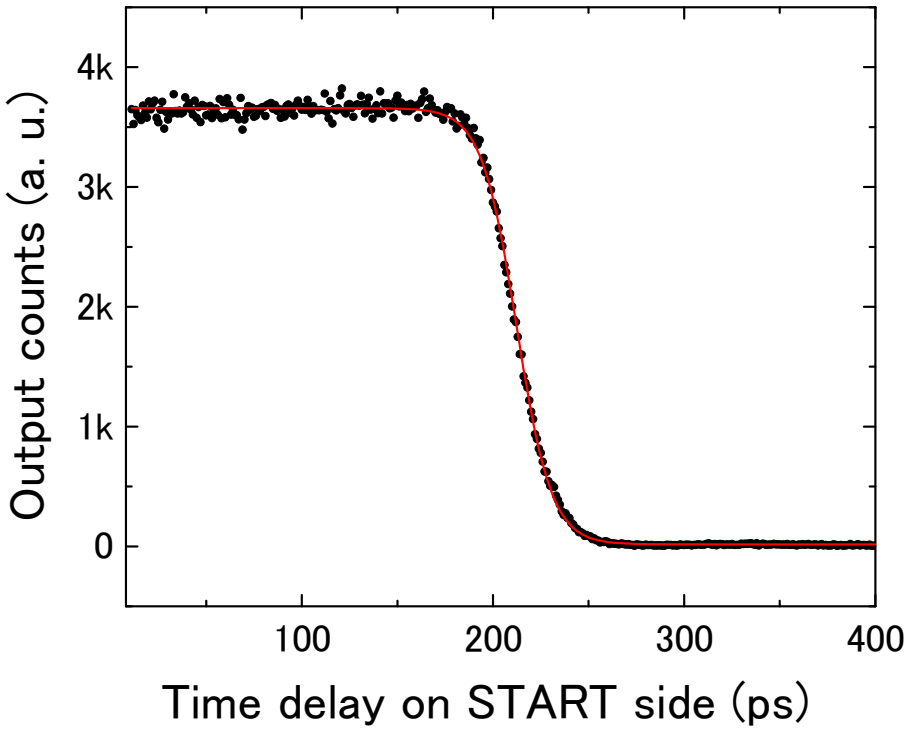

Fig. 2 Output counts number as a function of the time delay in photon arrival time on START side.

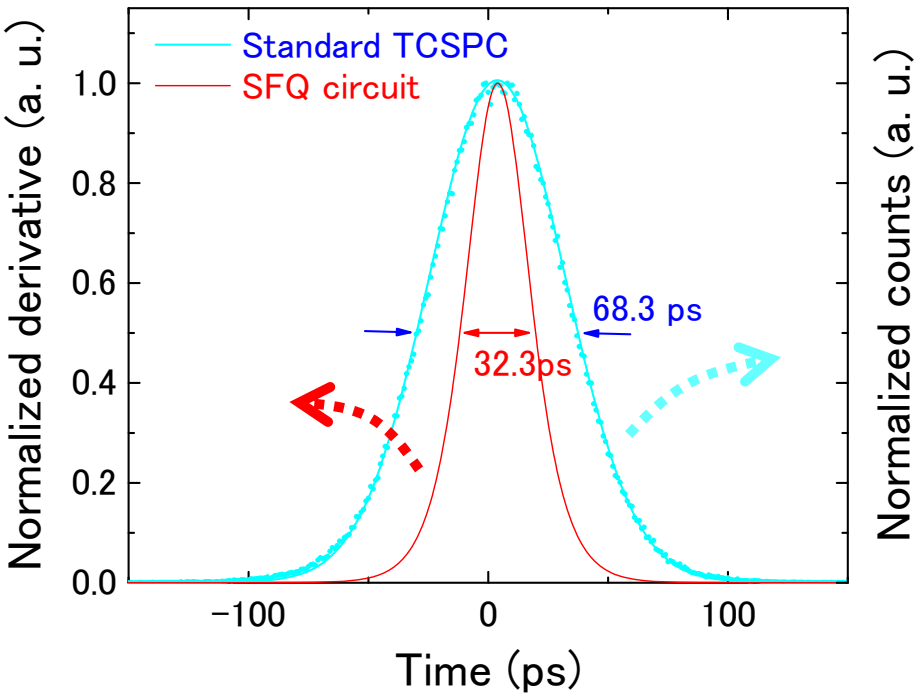

Fig. 3 Derivative curve was also obtained after sigmoidal fitting of the transition curve. The time correlated counting histogram between two detectors obtained by using the conventional TCSPC module is also shown for comparison.

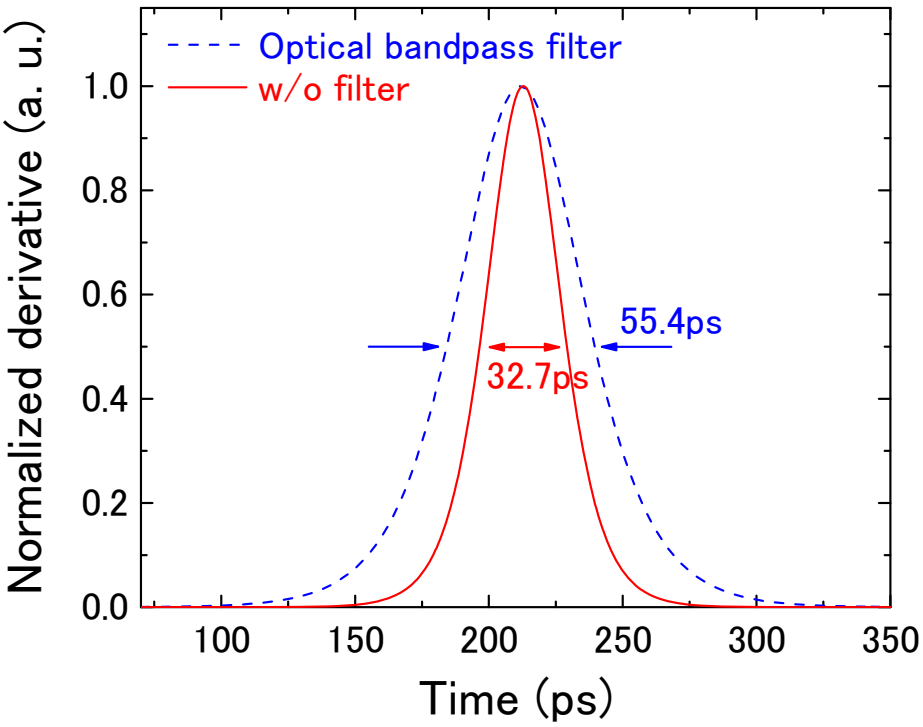

Fig. 4 Observed timing jitter characteristics with and without a wavelength bandpass optical filter.

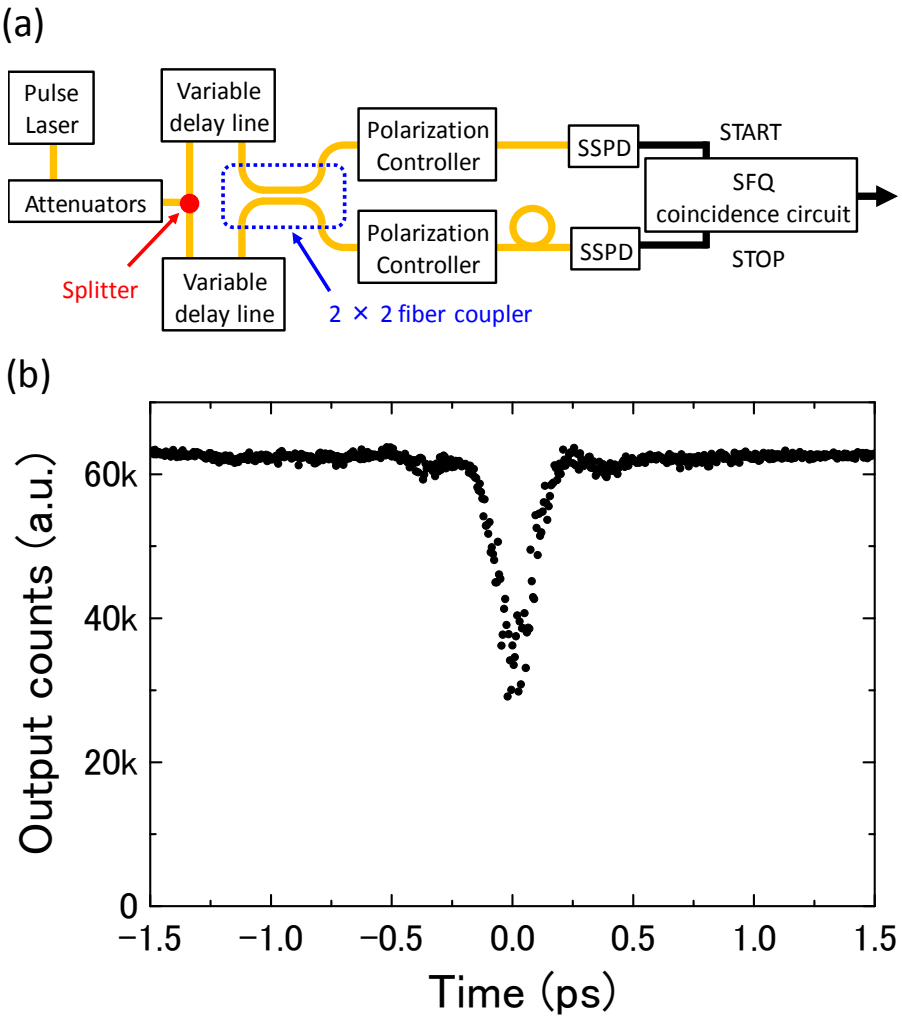

Fig. 5 (a) Schematic configuration of the photon source and coincidence photon counting system for HOM interference with classical photon source. (b) Observed two-photon interference using a classical light source.

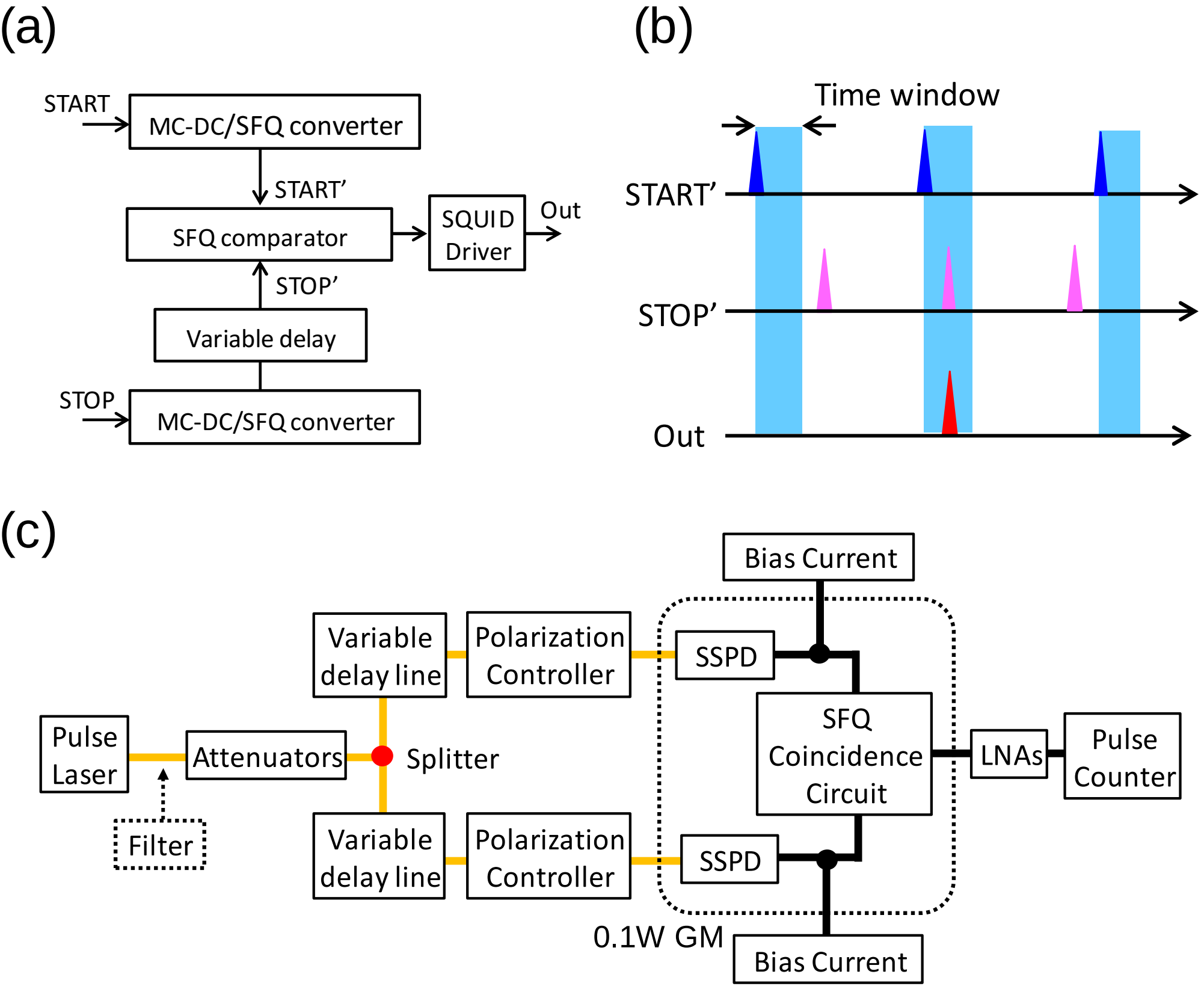
(a)
START
MC-DC/SFQ converter
START'
SFQ comparator
SQUID Driver
Out
STOP'
Variable delay
STOP
MC-DC/SFQ converter
(b)
Time window
START'
STOP'
Out
(c)
Bias Current
Variable delay line
Polarization Controller
SSPD
SFQ Coincidence Circuit
LNAs
Pulse Counter
Pulse Laser
Attenuators
Splitter
Filter
Variable delay line
Polarization Controller
SSPD
0.1W GM
Bias Current

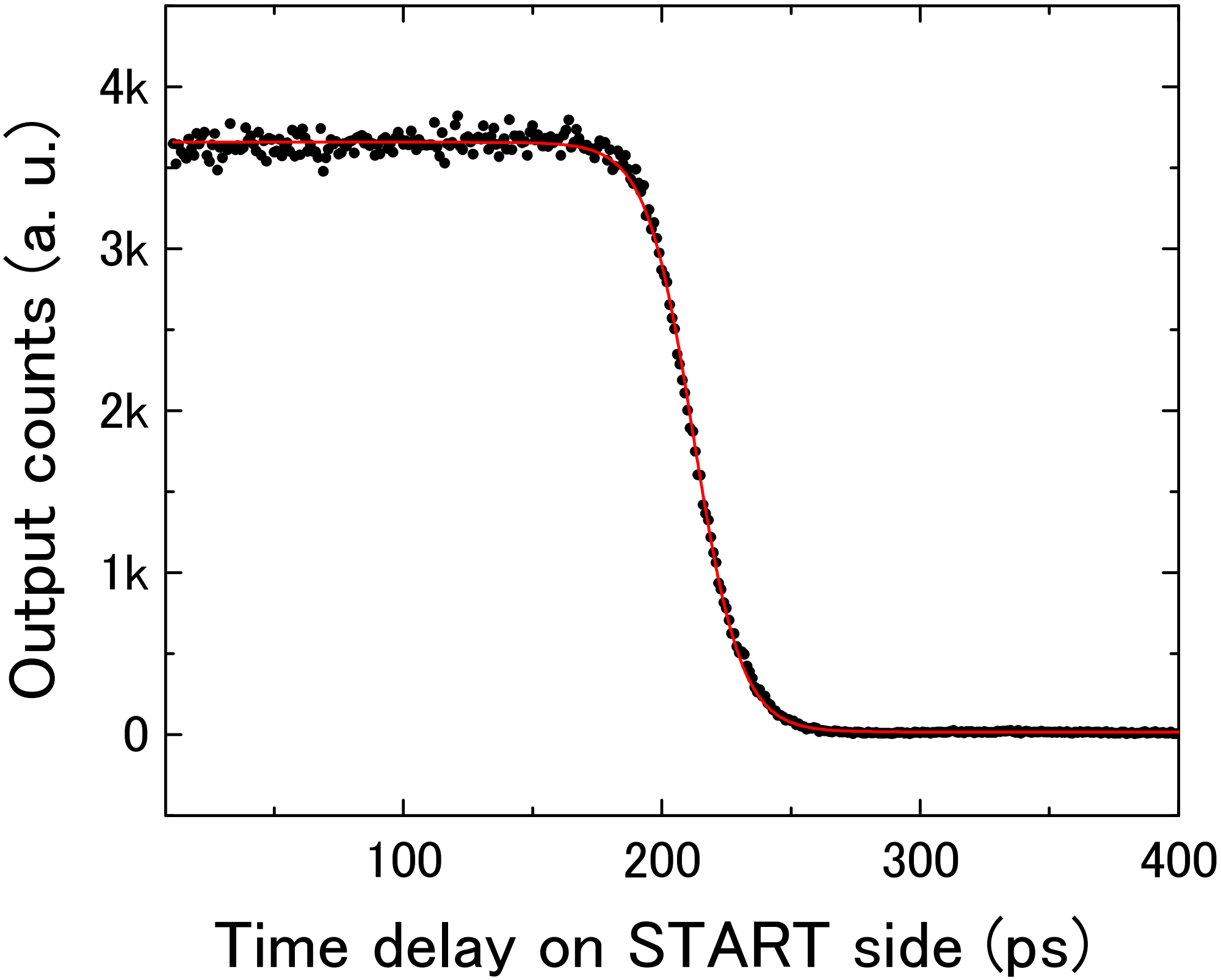
Output counts (a. u.)
4k
3k
2k
1k
0
100
200
300
400
Time delay on START side (ps)

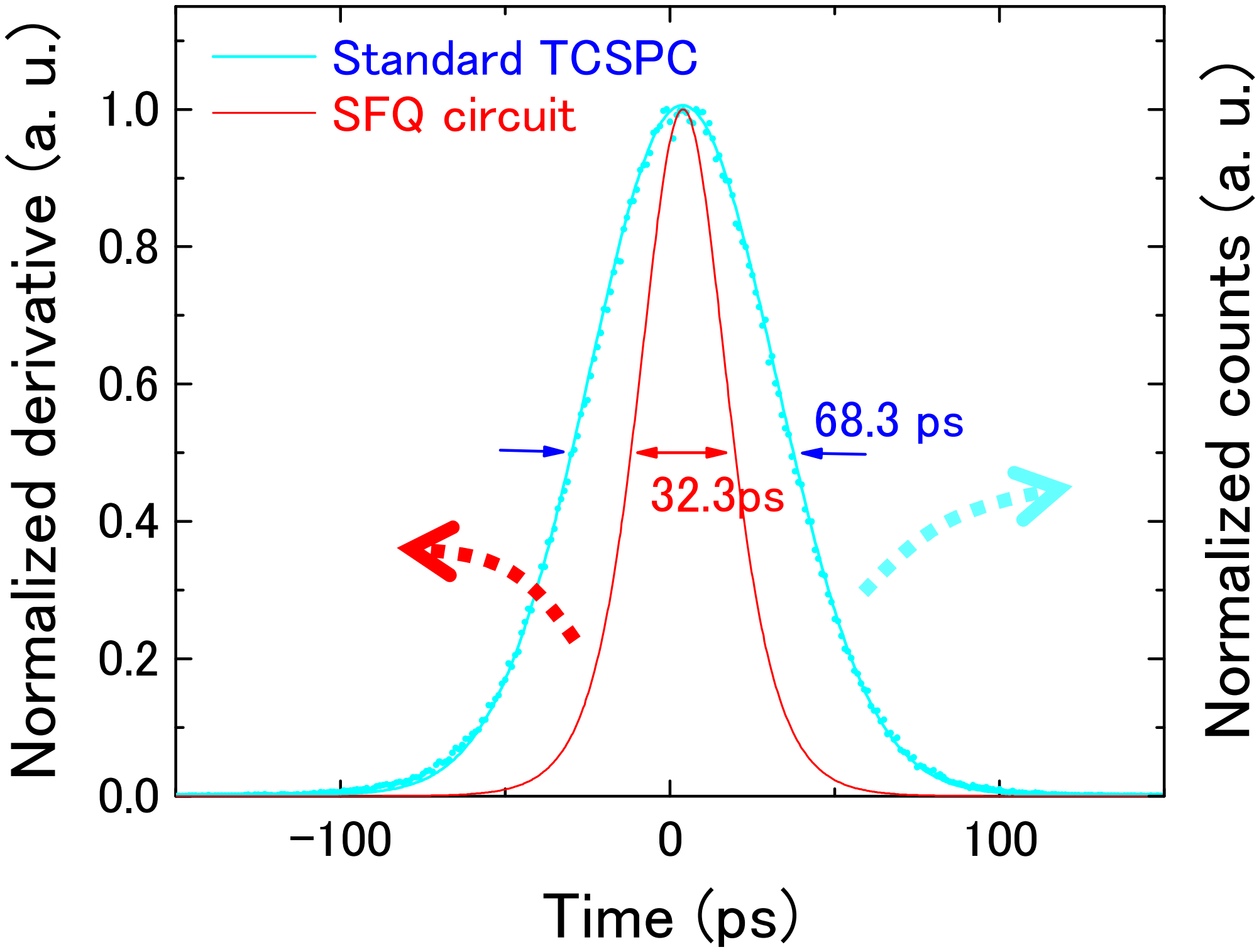
Standard TCSPC
SFQ circuit
68.3 ps
32.3ps
Normalized derivative (a. u.)
Normalized counts (a. u.)
Time (ps)
1.0
0.8
0.6
0.4
0.2
0.0
−100
0
100

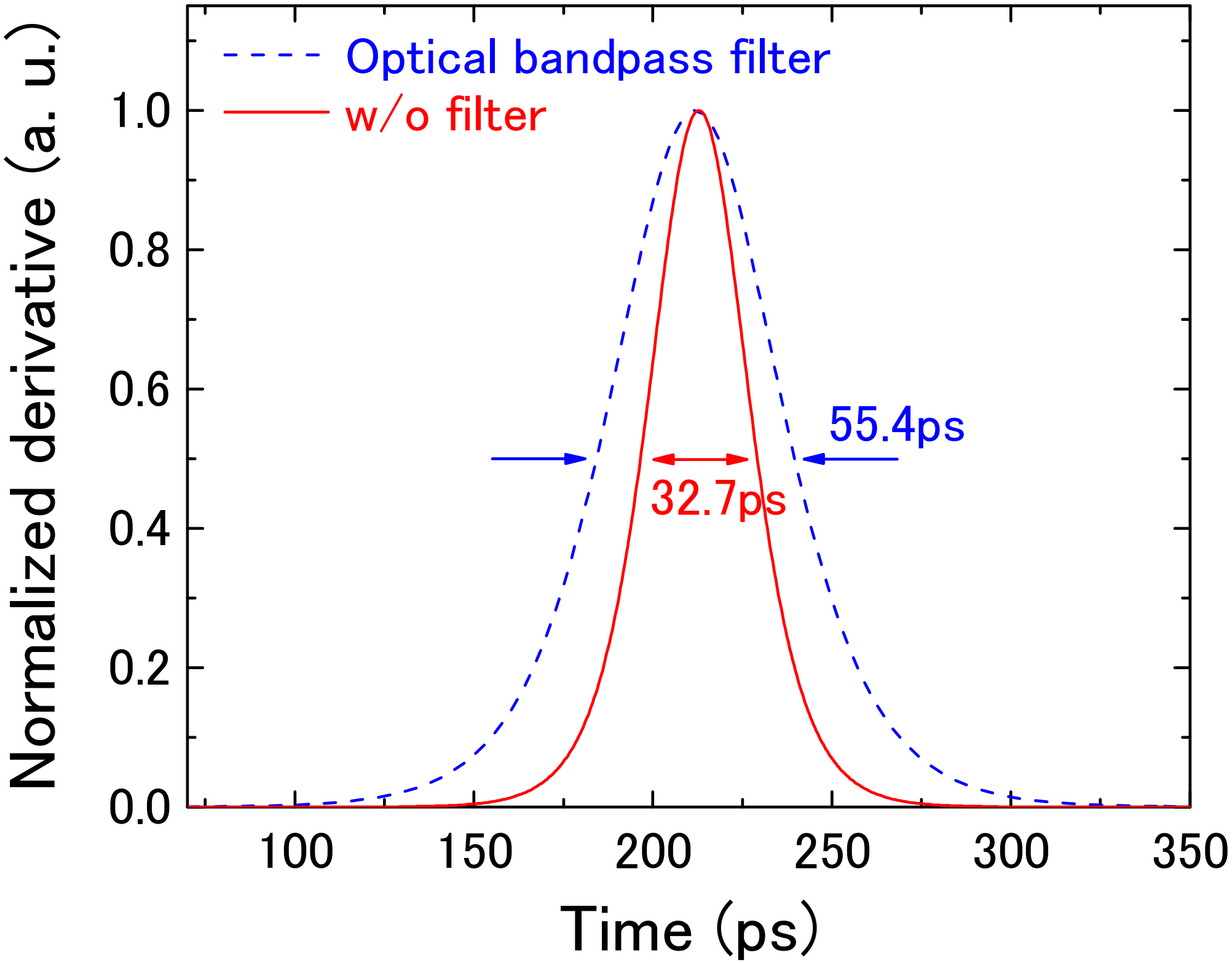
Optical bandpass filter
w/o filter
55.4ps
32.7ps
Normalized derivative (a. u.)
Time (ps)
0.0
0.2
0.4
0.6
0.8
1.0
100
150
200
250
300
350

(a)

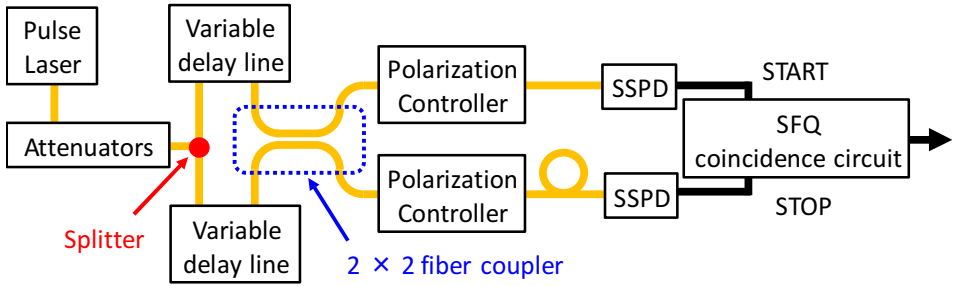
Pulse Laser
Attenuators
Variable delay line
Variable delay line
Splitter
2 × 2 fiber coupler
Polarization Controller
Polarization Controller
SSPD
SSPD
START
SFQ coincidence circuit
STOP

(b)

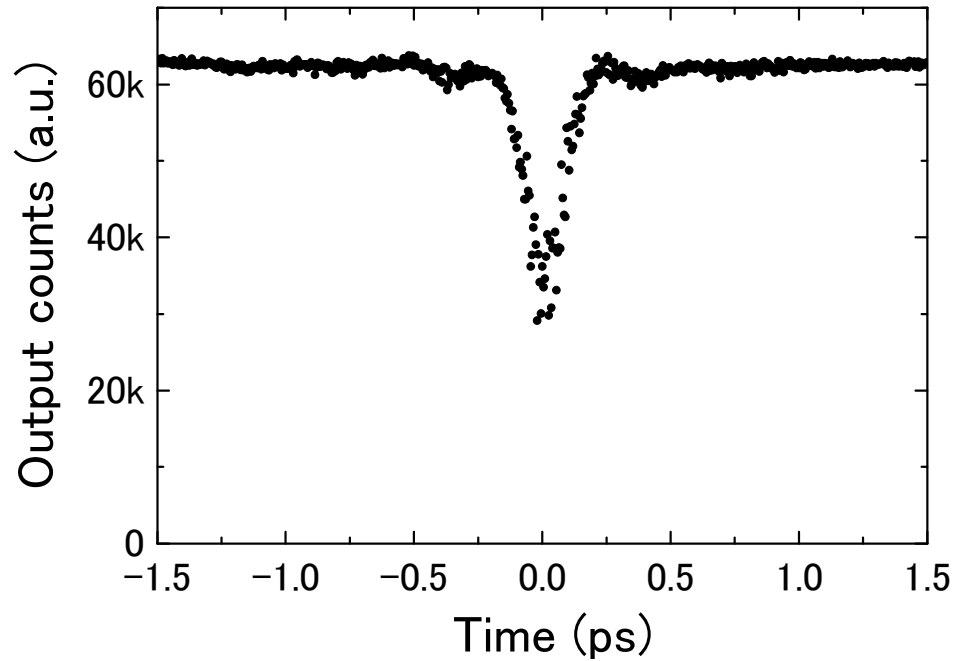
Output counts (a.u.)
60k
40k
20k
0
−1.5
−1.0
−0.5
0.0
0.5
1.0
1.5
Time (ps)